Highly efficient luminescence from hybrid structures of ZnO/multi-walled carbon nanotubes for

high performance display applications

Highly efficient luminescence from hybrid structures of ZnO/multi-walled carbon nanotubes for high performance display applications

Bipin Kumar Gupta[1,3]**, Vaneet Grover**[1,2]**, Govind Gupta**[1] **and V Shanker**[1]

[1] National Physical Laboratory (CSIR), Dr K S Krishnan Road, New Delhi-110012, India
[2] C.E.A.S.T., Department of Physics, Panjab University, Chandigarh-160014, India

E-mail: bipinbhu@yahoo.com and guptabgupta@nplindia.org

Abstract
We report an interesting observation on strong enhancement in green luminescence from hybrid ZnO/multi-walled carbon nanotubes (MWCNTs). The hybrid structures were synthesized via a high temperature sintering method. The strong green emission at 510 nm has been attributed to surface defects of ZnO, originating from interactions between ZnO and the MWCNT surface, which has been confirmed by high resolution transmission electron microscopy and x-ray photoelectron spectroscopy. Furthermore, the two-dimensional (2D) layer of this hybrid material shows a high degree of homogeneity and 82% transparency. Time resolved emission spectroscopy measurement shows a photoluminescence decay time in microseconds, which is suitable for making optoelectronic devices.

(Some figures in this article are in colour only in the electronic version)

1. Introduction

In the past decade, ZnO has generated great interest due to its potential applications in short-wavelength [1, 2], optoelectronic devices [1, 2], nanosensors [1, 2], field emission displays [1–3], field effect transistors [1, 2], optical switches [1, 2], electroluminescence devices [1, 2] and solar cells [1, 2] due to its wide band gap (e.g. ∼3.37 eV), high melting point (1975 °C) [3], good thermal stability, large exciton binding energy (∼60 meV) [4], low cost and ease of synthesis. Recently, ZnO hybrid structures have received much attention because of the ability to tune the optical properties by hybridizing them with different materials. At nanoscale, hybridization of ZnO with other materials alters the properties of both components which may give rise to functional materials with desirable properties. Few studies have been carried out in this direction in order to achieve the desired optical and electronic properties [5]. The co-operative structural and electronic interaction between ZnO and multi-

walled carbon nanotube (MWCNT) materials is the main reason behind the interesting enhancement in luminescent properties in the case of ZnO/MWCNT hybrid structure. Although there are several reports on ZnO/MWCNT hybrid structures, to date, only few attempts have been reported on the defect related enhancement in the luminescent properties of ZnO/MWCNT hybrid structures (theoretically as well as experimentally) [6, 7]. MWCNTs play a vital role in the observed enhanced green emission from ZnO/MWCNT hybrid structures due to surface diffusion and strong interaction between ZnO and MWCNT surfaces. Typically ZnO exhibits photoluminescence characteristics in the visible and UV regions. The UV emission at 370 nm is due to the radiative annihilation of excitons, while the green luminescence in ZnO arises from radiative recombination involving intrinsic defect centres such as the oxygen vacancies [8–11], interstitial oxygen [12, 13], Zn vacancies and interstitial Zn [14].

In the present work, we report an interesting observation of strong luminescence enhancement from hybrid structures obtained by admixing of various carbon nano-variants

---

[3] Author to whom any correspondence should be addressed.

(MWCNTs, graphite, charcoal, carbon wool) with ZnO. Structural/microstructural studies and x-ray photoelectron spectroscopy (XPS) results indicate that the enhanced green emission is due to a strong surface interaction between ZnO and MWCNTs through surface diffusion during the sintering process, which is responsible for increased surface defects on the ZnO/MWCNT interface. Moreover, we demonstrate fabrication of a uniformly distributed sodium hexametaphosphate (SHMP) capped ZnO/MWCNT hybrid layer having controlled particle density using the conventional spin-coating method followed by baking.

2. Experimental procedure

2.1. Synthesis of ZnO/MWCNT hybrid nanostructures

The synthesis of hybrid structures was performed in three successive steps. Initially, ZnO was synthesized by thermal oxidation of Zn dust (Qualigens fine chemicals, Ar grade, 300 mesh, 99.90% purity) at 800 °C under oxygen environment (Iolar Grade, 99.90% purity) at a gas flow rate of 500 sccm. MWCNTs was synthesized by a well-known spray pyrolysis method [15, 16]. Before using MWCNTs, special care was taken to make them free from iron as the presence of iron may alter the results (the iron acts as a quencher for luminescence) [17]. Purification was been carried out through a well-known heat treatment method [18, 19]. Other carbon nano-variants (graphite, charcoal and carbon wool) were of commercial grade (purity 99.98%) and used without further treatment. Finally, as-synthesized ZnO with carbon nano-variants was sintered at 750 °C in argon gas in a quartz tube. In order to have an idea of the feasibility of hybridization of various carbon nano-variants with ZnO for enhancing the luminescence property, we have used various forms of carbon nano-variants: MWCNTs, graphite, charcoal, and carbon wool. It has been observed that MWCNTs exhibit better luminescent properties with ZnO as compared to other carbon nano-variants. The PL intensity of hybrid structures increases with increasing the amount of MWCNTs up to a value of 0.75 mol% and the excess of MWCNTs shows blocking effects as the luminescence intensity decreases sharply [20]. Therefore optimum admixing of MWCNTs plays an essential role in the formation of hybrid structures (ZnO/MWCNTs) to enhance the luminescence.

2.2. Sample characterization

For phase identification, the structural characterization was performed using XRD (Rigaku: Miniflex, Cu Kα; λ = 1.5404 Å). The surface morphology and microstructural characterization were carried out by scanning electron microscopy (SEM, Model No. LEO 440), high resolution transmission electron microscopy (HRTEM, Model No. Technai G20-twin, 200 kV with super twin lenses having point and line resolutions of 0.144 nm and 0.232 nm, respectively) equipped with energy dispersive x-ray analysis (EDAX) facilities for elemental studies. The room-temperature photoluminescence (PL) spectra were recorded by PerkinElmer Luminescence Spectrometer (Model No. LS-55)
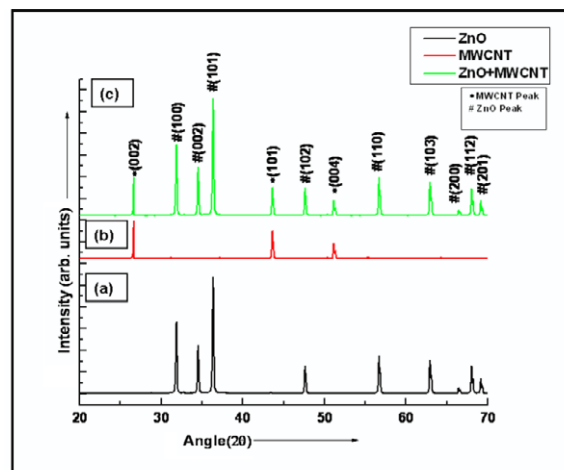
Figure 1. XRD patterns of the (a) ZnO, (b) pure MWCNT and (c) ZnO/MWCNT hybrid structures.

and time resolved photoluminescence (TRPL) was recorded using a microsecond xenon flash lamp, as the source of excitation, attached to Edinburgh Luminescence Spectrometer (Model No. F-900).

3. Results and discussion

Figures 1(a)–(c) show x-ray diffraction (XRD) patterns of three different samples i.e. ZnO, pure MWCNTs and ZnO/MWCNTs hybrid structures. The diffraction peaks for the ZnO samples were identified to be of ZnO wurtzite phase with space group *P*63*mc* as per JCPDS card No. 36-1451, which is shown in figure 1(a). The lattice parameters were estimated to be a = 3.2386 ± 0.0011 Å, c = 5.1768 ± 0.0008 Å. No diffraction peaks from any other impurities were detected. The particle size of the samples was estimated using Scherrer's formula, $D = 0.89\lambda/\beta\cos\Theta$, where D is the average diameter of the grains, λ(1.5404 Å) is the x-ray wavelength, β and Θ are the corrected full-width at half-maximum (FWHM) of the x-ray diffraction lines and the Bragg angle, respectively. The average crystallite size of ZnO powder was found to be ∼50 nm. Figure 1(b) represents the XRD pattern of pure MWCNTs and the estimated lattice parameters are a = 2.4623 ± 0.0013 Å, c = 6.4534 ± 0.0031 Å which matches well with JCPDS card No. 23-0064. In the present investigations, it can be noticed from figure 1(b) that the (002) peak of MWCNT is notably sharper compared to the usual MWCNT peak. This was because the MWCNT was used after purification, and in the purification process it was annealed at 500 °C. Hence re-crystallization has occurred and the (002) plane becomes ordered. Figure 1(c) shows the hybrid structure of ZnO/MWCNTs with lattice parameters a = 3.2174 ± 0.0034 Å, c = 5.1579 ± 0.0021 Å. The XRD result in figure 1(c) reveals that the lattice parameters slightly change as compared to as-synthesized ZnO. The very small variation in lattice parameters (second and third decimal place) in hybrid structures may be due to surface diffusion and the formation of a strong interface between ZnO and MWCNTs by an admixing and sintering process. In this process, the intrinsic

surface defects on ZnO surfaces were enormously enhanced, which is responsible for the strong green emission.

Figures 2(a)–(i) show a representative scanning electron micrograph (SEM) of as-synthesized ZnO, pure MWCNT, ZnO/MWCNT hybrid structures, pure graphite ZnO/graphite hybrid structures, pure charcoal, ZnO/charcoal hybrid structures, pure carbon wool, ZnO/carbon wool hybrid structures respectively. It can be seen clearly in figure 2(a) that the as-synthesized ZnO powder is composed of almost spherical particles, which is further confirmed by TEM. Figure 2(b) represents the SEM image of purified MWCNTs. The average diameter and length of the MWCNTs are in the ranges ∼30 nm and 20 μm respectively. The SEM results reveal that the high crystalline strongly coupled interface is formed only in ZnO/MWCNT hybrid structures and not in the other carbon nano-variants as shown in figure 2(c). In the other carbon variant cases, the crystallinity of ZnO has been affected and destroyed, which can be easily seen in figures 2(e), (g) and (i), which may also influence the luminescent properties. The direct evidence of the interface formation of ZnO nanoparticles with MWCNTs is given by the TEM and HRTEM in figures 2(j)–(l) respectively. Figure 2(j) exhibits the as-synthesized ZnO samples, the result of TEM reveals that most of the ZnO nanoparticles are composed of spherical shapes, and the inset shows a typical HRTEM image. The precise observation and estimated interspacing is 2.70 Å which reflects the (100) plane. This represents the wurtzite structure of ZnO. Figure 2(k) shows the typical TEM image of pure MWCNTs and in inset represents the HRTEM image of pure MWCNTs. From HRTEM, the estimated interspacing is 3.43 Å which reflects the (002) plane. Further, to understand the interaction between the surfaces, TEM, EDAX HRTEM studies have been carried out for the ZnO/MWCNT hybrid structure and the results are shown in figures 2(l)–(n) and 3(a), respectively. Figure 2(l) exhibits clearly the interface formation between ZnO and MWCNT surfaces and figure 2(m) shows the selected area electron diffraction (SAED) pattern. The SAED pattern has been taken on the interface of the ZnO and MWCNTs, the SAED results exhibit the (100), (101) reflections of ZnO and (002) reflection of MWCNT which confirms the interface formation. EDAX was carried out to further probe the elemental composition of the interface (marked as a red circle in the inset) of ZnO/MWCNT surfaces as shown in figure 2(n). It reveals the presence of Zn, O, Cu and C on the surface of the hybrid materials, which again confirms the existence of ZnO interface formation with MWCNTs. The C signal originates from MWCNTs and the Cu signal comes from the copper grid. Figure 3(a) represents a typical HRTEM image of the ZnO/MWCNT hybrid structure. The lattice fringes, the interface between ZnO spherical nanoparticles and the outmost shell of the MWCNTs are clearly visible in figure 3(a), which suggests that a well-developed interface is formed between the ZnO and MWCNTs because of the high temperature sintering method used. The lattice fringe spacings of the ZnO and MWCNTs are indexed as (100) and (002) planes of reflections with a slight change in the *d*-spacing of 2.70 Å and 3.43 Å respectively. The two types of phases can be clearly seen in figure 3(a). Some of this region is expected to

be highly defective in order to release a large amount of strain at the interface [21].

The chemical composition and further information on the formation of ZnO/MWCNT hybrid structures were derived from x-ray photoelectron spectroscopy (XPS) studies. The measurements were carried out in an ultra-high vacuum chamber (P HI1257) with a base pressure of 4×10^{-10} Torr. The system was equipped with a high resolution hemispherical electron energy analyser (279.4 nm diameter) with 25 meV resolution. XPS studies of ZnO/MWCNTs and ZnO/graphite have been carried out to analyse the nature of the interface formation and surface diffusion. Gold has been deposited on a portion of the sample and has been taken as a standard in order to take care of the shifts due to charging, etc. Figure 3(b) shows the XPS results obtained from ZnO/MWCNTs and ZnO/graphite. The survey spectra in figure 3(b) exhibit sharp peaks of C 1s (280.40 eV), O 1s (527.97 eV), Zn 2p3/2 (1021.30 eV) and Zn 2p1/2 (1044.40 eV) for ZnO/graphite. The observed values for ZnO/MWCNTs are C 1s (280.16 eV), O 1s (527.50 eV), Zn 2p3/2 (1021.05 eV) and Zn 2p1/2 (1044.13 eV). It should be noticed that the XPS peak positions for C 1s, O 1s and Zn 2p shift from the original values for C 1s (284.60 eV), O 1s (531.60 eV), Zn 2p3/2 (1021.45 eV) and Zn 2p1/2 (1044.55 eV) [5] due to interface formation and charge accumulation on the interface. The inset of figure 3(b) shows the deconvoluted C 1s spectra of ZnO/MWCNTs and ZnO/graphite where the spectra reveal that the surface interaction of Zn with MWCNT carbon is two times higher than the surface interaction of Zn with graphitic carbon. Similar studies have been carried out for other carbon nano-variants and it has been observed that MWCNTs form a better interface with ZnO than any other kind of carbon nano-variant. Because of the strong interface formation between ZnO/MWCNTs, large surface defects were generated compared to any other carbon nano-variants, which has been further confirmed by photoluminescence (PL) studies.

PL is an essential direct optical probe for the determination of electronic energy band structure and surface defect analysis. It can provide useful qualitative information about the interaction of free electrons on the surface of MWCNTs with ZnO. Figure 4(a) shows the broad green emission peaking at 510 nm (with colour coordinate, $x = 0.2225$, $y = 0.4004$) and the inset of figure 4(b) shows the excitation spectra of ZnO/MWCNTs at 376 nm which is slightly shifted from the band edge of ZnO 380 nm (3.26 eV). The mechanism of the defect related electron–hole recombination process in ZnO has been intensively investigated, yet it remains a controversial subject [5]. Among the different mechanisms proposed to explain the visible luminescence, oxygen vacancies have been widely considered as the most probable candidate [8–11]. In the present study, we have used various carbon nano-variants to introduce intrinsic defects in ZnO in order to enhance the green emission. We propose that carbon plays a very crucial role in enhancing the green emission of the ZnO/MWCNT hybrid structure. The strong interface formed through admixed ZnO and MWCNT surfaces, creates the defect level necessary for green emissions. It was observed that there were no emission peaks observed in the pristine carbon
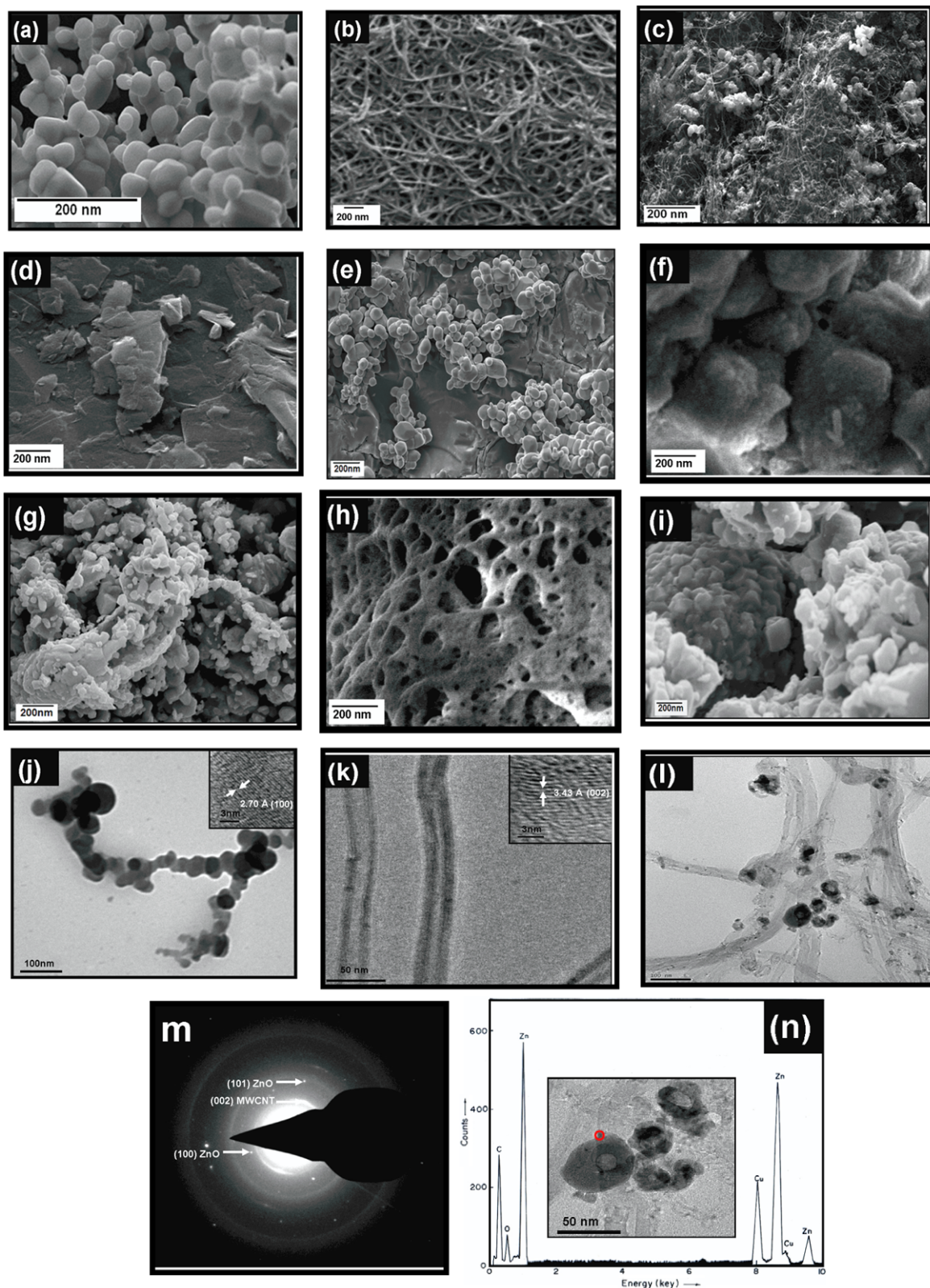
Figure 2. (a)–(i) SEM images of (a) as-synthesized ZnO, (b) pure MWCNTs, (c) ZnO/MWCNT hybrid structures, (d) pure graphite, (e) ZnO/graphite hybrid structures, (f) pure charcoal, (g) ZnO/charcoal hybrid structures, (h) pure carbon wool, (i) ZnO/carbon wool hybrid structures respectively. (j) Typical TEM image of pure ZnO, and the inset shows the HRTEM image, (k) typical TEM image of pure MWCNTs, and the inset shows the HRTEM image of pure MWCNTs. (l) Represents the TEM image of the ZnO/MWCNT hybrid structure. (m) Exhibits the SAED pattern of the ZnO/MWCNT hybrid material. (n) Shows the EDAX spectrum of the ZnO/MWCNT hybrid structure; the inset shows the TEM of the ZnO/MWCNT hybrid structure.
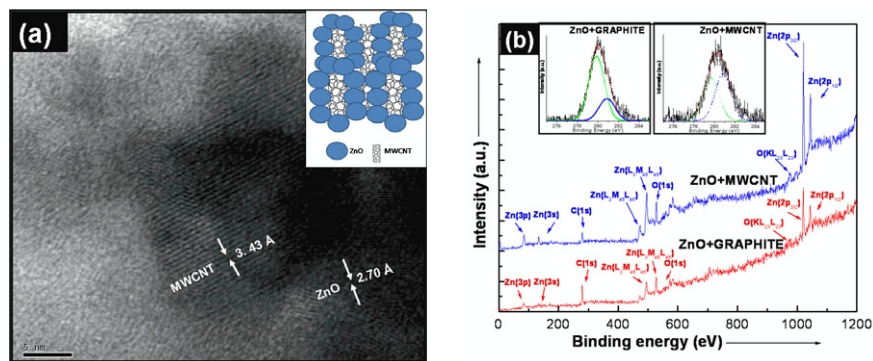
Figure 3. (a) HRTEM image of ZnO/MWCNTs, the inset shows the interaction between the ZnO and MWCNT surfaces, (b) XPS survey scan spectra of ZnO/MWCNTs and ZnO/graphite recorded with Al Kα ($h\nu = 1486.6$ eV).
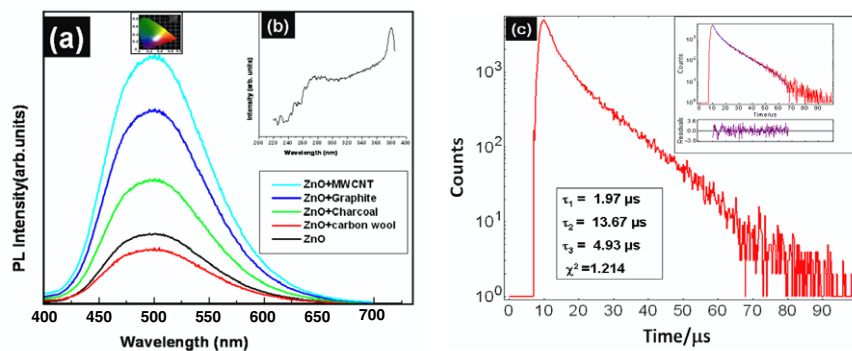
Figure 4. (a) Steady-state photoluminescence emission spectra of ZnO/carbon nano-variants recorded at 376 nm, (b) shows the corresponding PLE spectra of ZnO/MWCNTs, (c) time resolved photoluminescence decay profile of the ZnO/MWCNT hybrid structure at room temperature while monitoring the emission at 510 nm at an excitation of 376 nm. The inset shows the life time data and the parameters generated by the exponential fitting.

variant at 376 nm excitation. The carbon variant was excited at 246 nm and gave emission at 398 nm. So, it is clear that the emission was observed from the ZnO/carbon variant hybrid. We have also observed an interesting result in PL spectra which is shown in figure 4(a). ZnO/MWCNTs have higher luminescence characteristics than other carbon nano-variants (graphite, charcoal, and carbon wool). The probable reason behind the strong luminescence in ZnO/MWCNTs may be the higher interfacial area provided by MWCNTs to ZnO than other carbon nano-variants. Higher surface to volume ratio leads to higher concentration of defects on the ZnO surfaces. Besides this, the availability of delocalized π electrons is more on the surfaces of MWCNTs as compared to other carbon variants. We have also studied different shapes of ZnO, but spherical shaped ZnO shows the strongest luminescence. The possible mechanism for strong green emission enhancement may be the recombination of Vo$^+$ from the ZnO surface and free electrons from MWCNTs (with photoexcited holes in the valence band).

To evaluate the usefulness of luminescence of ZnO/MWCNT hybrid materials, the intensity temporal behaviour is investigated. Figure 4(c) shows the time resolved luminescence of ZnO/MWCNT hybrid structures. The decay was recorded for the transition at 510 nm emission and 376 nm excitation by a time-correlated single photon counting technique. The PL decay curve was measured with a xenon flash lamp as a source of excitation. Figure 4(c) clearly indicates that the

luminescence life time for ZnO/MWCNTs at 510 nm emission was delayed for $\sim$14 μs ($\tau 1 = 1.97$ μs, $\tau 2 = 13.67$ μs, $\tau 3 = 4.93$ μs). The life time data were very well fitted exponentially and the parameters generated from the fitting are listed in the inset of figure 4(c).

In order to produce transparent and aqueous-stable hybrid (ZnO/MWCNT) colloidal solution from the as-synthesized hybrid material (ZnO/MWCNTs), we have adopted a simple encapsulation method [22]. Initially, SHMP from Sigma-Aldrich was taken and dissolved in de-ionized (DI) water at a molar concentration of 2%. After complete dissolution of SHMP, 120 mg hybrid material was added to 50 ml of SHMP solution followed by vigorous stirring at room temperature for around 30 min. Then ethanol (2 ml) was added and the mixture was kept in an ultrasonic bath for about 2 h for proper encapsulation by the phosphate matrix. Finally, the capped hybrid particulate was collected by centrifuging at $\sim$8000 rpm for 15 min. 0.60 mg cm^{-3} of the obtained precipitate was re-dispersed in fresh DI water at room temperature ($\sim$27 °C) to make it an aqueous-stable and highly transparent liquid ($>$82% in the visible region). Figure 5(a(i)) shows a transparent optical image of the hybrid colloid under ambient light. The transparent colloid shown in figure 5(a(ii)) exhibits strong green luminescence under 370 nm wavelength illumination. The transparent layer was dried by vacuum baking. Figure 5(b) shows the transparent layer of uniformly distributed hybrid ZnO/MWCNTs capped with SHMP having controlled particle
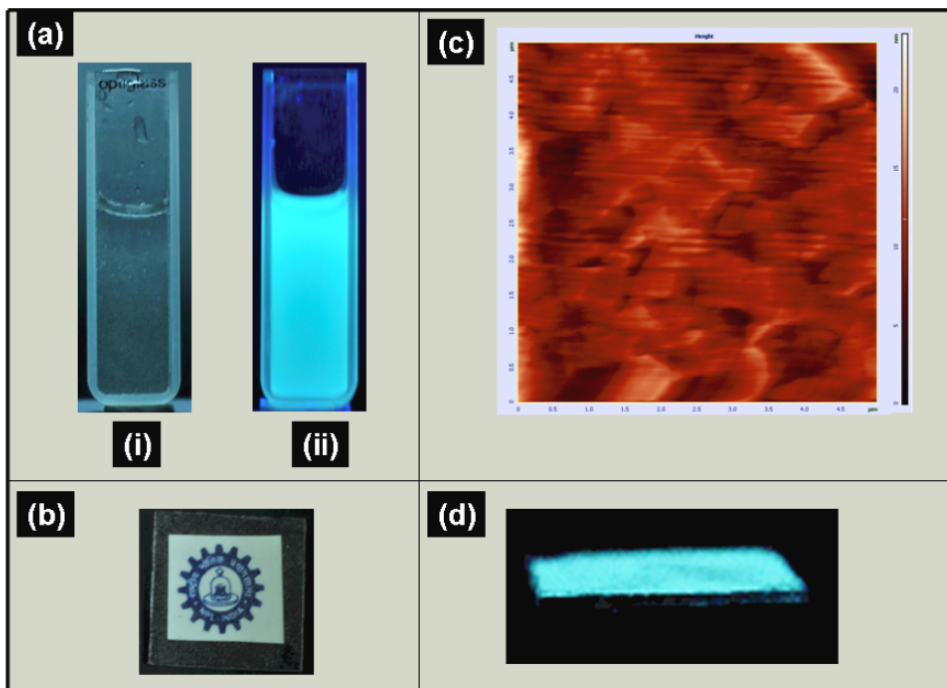
Figure 5. Typical photograph of a quartz-cuvette containing ZnO/MWCNT hybrid material dispersed in SHMP: (a(i)) depicts the transparency of the colloid under room light, (a(ii)) shows strong green emission at 510 nm under UV 370 nm light, (b) transparent layer showing 82% transparency, (c) AFM image showing uniformity of the film formed from ZnO/MWCNT hybrid material, (d) when the transparent layer is exposed to 370 nm light it shows strong green emission.

density. Atomic force microscopy (AFM) results reveal that the surface is highly uniform as shown in figure 5(c). Upon exposure to 370 nm light, the layer showed a strong green emission as shown in figure 5(d). Thus, the results are quite suitable for the fabrication of optoelectronic devices such as electroluminescence devices, invisible luminescent security ink, ZnO based diodes, as well as many other applications.

4. Conclusions

In summary, we have successfully synthesized and established the strong green luminescent properties of ZnO/MWCNT hybrid structures which can be useful for various types of applications. The photoluminescence intensity reveals that ZnO/MWCNTs has higher luminescence intensity compared to other carbon nano-variants due to its higher surface to volume ratio. We have also demonstrated that a transparent layer of hybrid material having high degree of homogeneity and 82% transparency can be formed. Time resolved emission spectroscopy measurement indicates a PL decay time in the range of $\sim$14 μs, which is suitable for making optoelectronic devices.

Acknowledgments

References

[1] Lim J-H, Kang C-K, Kim K-K, Huang D-K and Park S-J 2006 *Adv. Mater.* **18** 2720
[2] Hu G, Gong H, Chor E F and Wu P 2006 *Appl. Phys. Lett.* **89** 251102
[3] Gupta B K, Haranath D, Chawla S, Chander H, Singh V N and Shanker V 2010 *Nanotechnology* **21** 225709
[4] Kong X Y, Ding Y, Yang R and Wang J L 2004 *Science* **303** 1348
[5] Zhang R, Fan L, Fang Y and Yang S 2008 *J. Mater. Chem.* **18** 4964
[6] Lu Y H, Hong Z X, Fengg Y P and Russo S P 2010 *Appl. Phys. Lett.* **96** 091914
[7] Hu Y and Chen H-J 2008 *Mater. Res. Bull.* **43** 2153
[8] Riehl N and Ortman O 1952 *Z. Electrochem.* **60** 149
[9] Kasai P H 1963 *Phys. Rev.* **130** 989
[10] Kroger F A and Vink H J 1954 *J. Chem. Phys.* **22** 250
[11] Prosanov I Y and Politov A A 1995 *Inorg. Mater.* **31** 663
[12] Hahn D and Nink R 1965 *Phys. Condens. Mater.* **3** 311
[13] Liu M, Kitai A H and Mascher P 1992 *J. Lumin.* **54** 35
[14] Bylander E G 1978 *J. Appl. Phys.* **49** 1188
[15] Mayne M, Grobert N, Terrones M, Kamalakarn R, Ruhle M, Kroto H W and Walton D R M 2001 *Chem. Phys. Lett.* **338** 101
[16] Gupta B K, Shanker V, Arora M and Haranath D 2009 *Appl. Phys. Lett.* **95** 073115
[17] Borse P H, Deshmukh N, Shinde R F, Date S K and Kulkarni S K 1999 *J. Mater. Sci.* **34** 6087
[18] Ebbesen T W, Ajayan P M, Hlura H and Tanigaki K 1994 *Nature* **367** 519
[19] Hou P-X, Liu C and Cheng H M 2008 *Carbon* **46** 2003
[20] Kim S, Shin D H, Kim C O, Hwang S W, Choi S-H, Ji S and Koo J-Y 2009 *Appl. Phys. Lett.* **94** 213113
[21] Gupta B K, Haranath D, Saini S, Singh V and Shanker V 2010 *Nanotechnology* **21** 055607
[22] Pan L, Lew K K, Redwing J M and Dickey E C 2005 *Nano Lett.* **5** 1081